

The American Journal of Human Genetics, Volume 87

Supplemental Data

Mechanisms of Genomic Instabilities Underlying

Two Common Fragile-Site-Associated Loci,

***PARK2* and *DMD*, in Germ Cell and Cancer Cell Lines**

Jun Mitsui, Yuji Takahashi, Jun Goto, Hiroyuki Tomiyama, Shunpei Ishikawa, Hiroyo Yoshino, Narihiro Minami, David I. Smith, Suzanne Lesage, Hiroyuki Aburatani, Ichizo Nishino, Alexis Brice, Nobutaka Hattori, and Shoji Tsuji

Figure S1. Six Independent Deletions Occurring Simultaneously in One Cancer Cell Line

Scan data of array CGH analysis of one cancer cell line with 6 independent deletions occurring simultaneously. The horizontal axis represents the nucleotide position. The vertical axis represents \log_2 (case/reference signal intensities) on array CGH. Dots of \log_2 (case/reference signal intensities) of more than 0 are shown in red and those of less than 0 are shown in green. Black double arrows represent the length of each deletion.

Multiple deletions occurring independently in *PARK2* in one cancer cell line (COLO320)

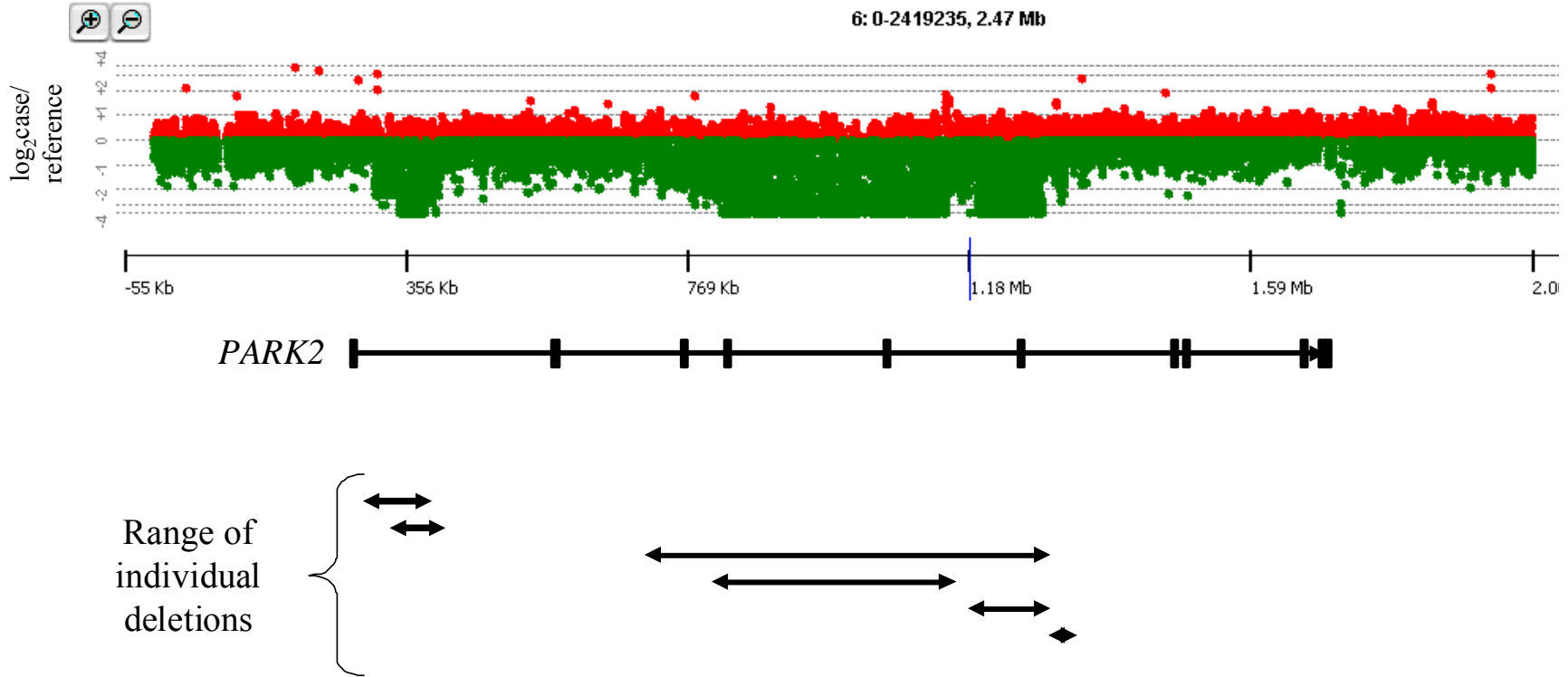
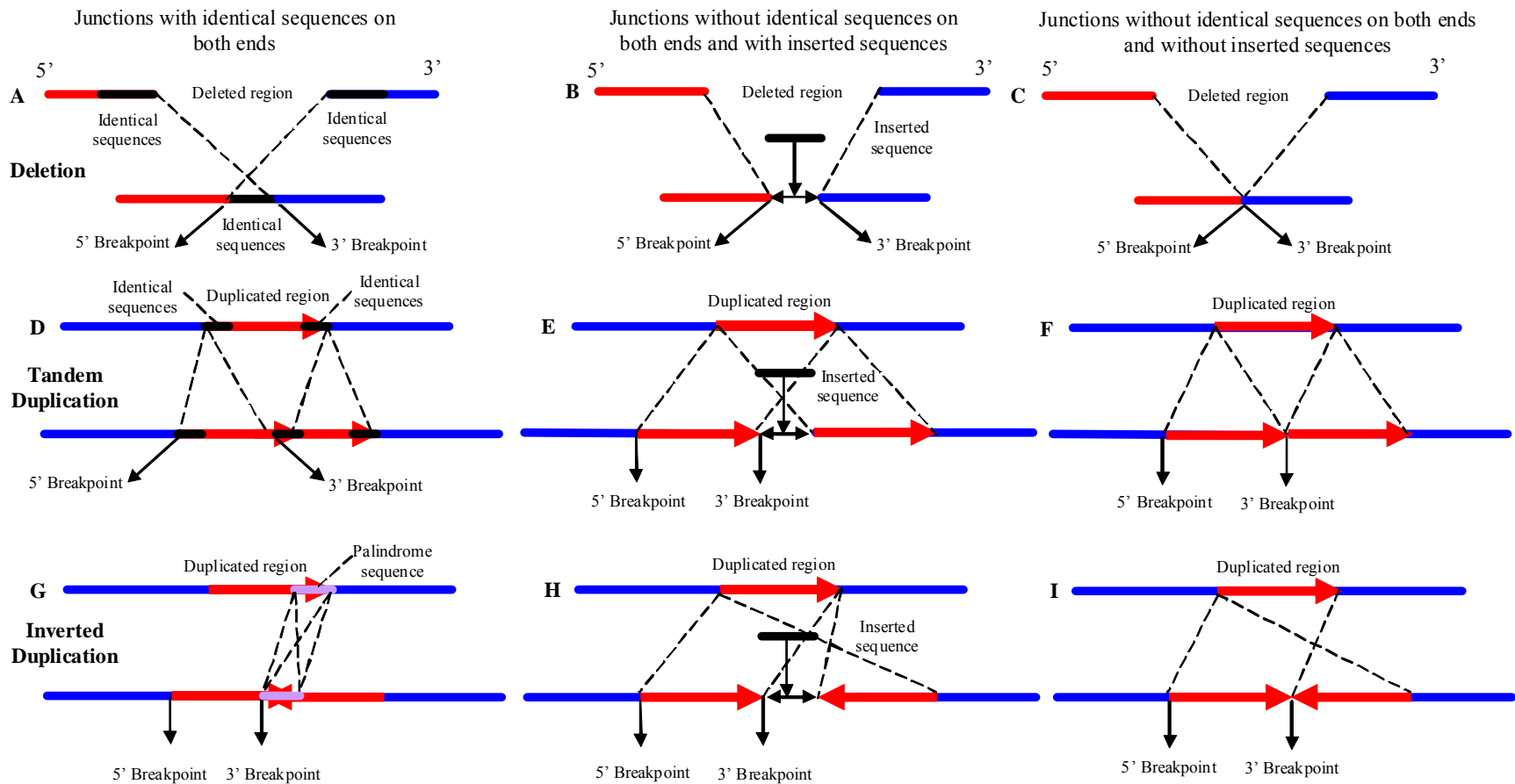


Figure S2. Definitions of Nucleotide Positions of Breakpoints and Schemes of Three Types of Junction

Scheme 1: junctions with identical sequences on both ends. Scheme 2: junctions without identical sequences on both ends and with inserted sequences. Scheme 3: junctions without identical sequences on both ends and without inserted sequences. In each scheme, nucleotide positions of breakpoints are indicated. The numbers of breakpoints in patients with AR-JP, patients with DMD/BMD, and cancer cell lines are shown below.

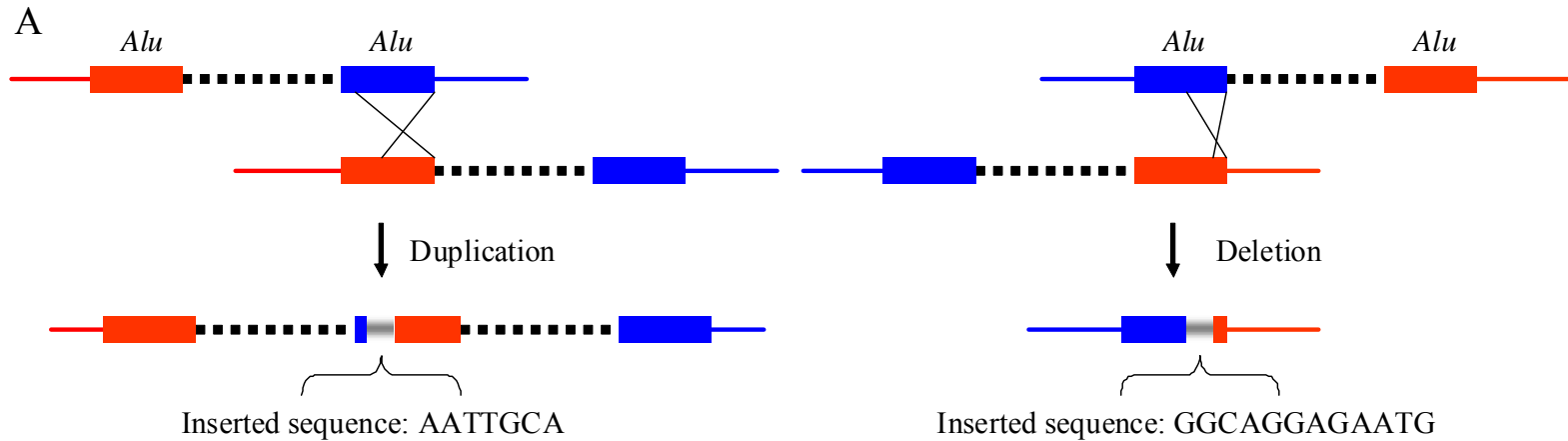
Definitions of nucleotide sequence positions of breakpoints



Sample sources	A	B	C	D	E	F	G	H	I	Total
<i>PARK2</i> (Patients with AR-JP)	94	47	7	9	5	0	0	0	0	162
<i>PARK2</i> (Cancer cell lines)	20	9	2	0	1	0	0	0	0	32
<i>DMD</i> (Patients with DMD/BMD)	120	48	15	9	5	0	0	0	0	197
<i>DMD</i> (Cancer cell lines)	3	2	1	0	0	0	0	0	0	6

Figure S3. Scheme of Junctions Forming Partial Chimeric *Alu/Alu* with Inserted Sequences of 7 bp and 12 bp at Their Junctions

- A. Both ends of breakpoints are embedded in *Alu* sequences and partial chimeric *Alu/Alu* sequences are formed at the breakpoint junctions. The blue and red boxes represent *Alu* sequences of the left and right sides of junctions, respectively. Light gray boxes are deleted *Alu* sequences from chimeric *Alu/Alu* junction segments. There are inserted sequences in the regions of light gray boxes.
- B. Specific sequences are shown below for junctions forming partial chimeric *Alu/Alu* sequences. The nucleotide sequences of the segments are in the same colors as those in part A. Double arrows denote connections of sequences of both sides.



B Duplication of “Chromosome 6: 162,253,158 - 162,123,917” with inserted sequence “AATTGCA” at its junction

```

TTTATTTTTTTT<---AATTGCA--->GGCATGATC
|||||
TTTATTTTTTTT<---AATTGCA--->GGCATGATC
|||||
TCGGCTCACTGCAACCTTGGCCTCCCAGGTTCAAGTGATTCTCCTGCCTCAGCCTCCCAA
TCCA<CTCACTGCAACTGCTGCCTCCTGGGTTCAAGCAATTTCTCCTGCCTCAGCCTCCCAA
GTAGCTGGGACTACAGGTGCATGCCACCATGCCCTGCTAATTTTTGTATTTTTAGTAGAG
GTAGTTGGGATTACAGGTGCCCGCCATCACACCCGGTAATTTTGTATTTTTAGTAGAG
ATGGGGTTTCGCCATGTTAACCAGGCTGTCTCTAACTCCTGACCTCAGGTGATCCGCC
ACGGTGTTTTACCATGTTGACCAGGCTGGTACGAACCTCTGACCTCAGGTGATCTGTCC
ACCTCAGCCTCCCAAAGTGCITGGGATTACAGGCATGAGCCACTGCACCTGGCC
GCCTCGCCCTCCCAAAGTGCITGGGATTACAGGCATGAGCTACCATGCCTGGCC
    
```

Deletion of “Chromosome X: 32,076,013 - 31,762,546” with inserted sequence “GGCAGGAGAATG” at its junction

```

GGCCGGGTGCGGTGGCTCACGCCTGTAATCCAGCACCTTTGGGAGGCCGAGCGGGCTGA
GGCTGGGCATGGTGGCTCATGCCTATAATCCAGCACCTTTGCGAGGCCGAGGCAGGCGGA
TCA--CGAGGTCAGGAGATCGAGACCATCCTGGCGAACACGGTGAAACCCCGTCTCTACT
TCACCTGAGGTCAGGAGTTTCGAGACCTGCCTGGCCAAATGGTGAAACCCGTCTCTACT
AAAAATATAAAAAATTAGCCTGGCGTGGTAGTGGGTGCCTGTAGTCCAGCTACTCGGGA
AAAAATAT-GAAAATGAGCCAGCTGTGGTGGCAGGCCTGTAATCCAGCTACTTGGA
GGCTGAGGCAGGAGAATGGCGTG
GGCTGAGGCAGGAGAATCACTTG<---GGCAGGAGAATG--->GAGATCGC
GCCACTGCACTCCAGCCTGGGTGACA-GAGCGAGACTCCATCTCAAAA
GCTGTGCACTCCAGCCTGGGCGACAGGCGAAACTCCGTCTCAAAA
    
```


Figure S6. Schematic Representation of Physical Relationships between Genes Located in CFSs and large LADs

Physical maps of genes located in CFSs (*FHIT*, *WWOX*, *GRID2*, and *LARGE*) and chromosomal R/G bands are shown. Box filled with diagonal lines denotes position of LADs. The genes located in CFSs are embedded in large LADs spanning several Mb (approximately 1.7 to 4.7 Mb)

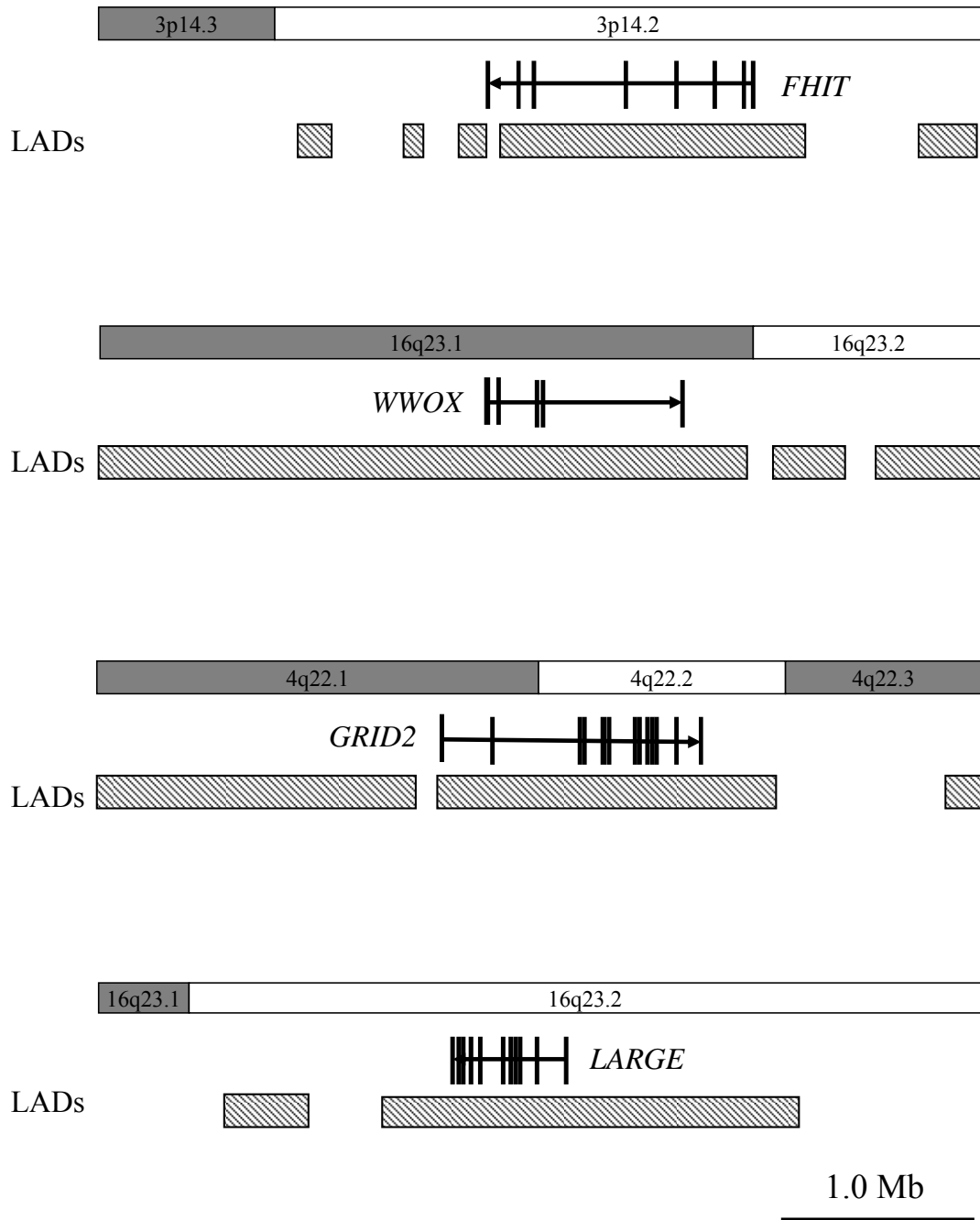


Table S1. List of Cancer Cell Lines

Cell line	Histology				
22Rv1	Prostate cancer	HLF	Liver cancer	PANC-1	Pancreatic cancer
A2058	Melanoma	Hs578T	Breast cancer	PC-3	Prostate cancer
A431	Skin cancer	HT1080	Fibrosarcoma	PK-0	Pancreatic cancer
A549	Lung cancer	HT1197	Bladder cancer	PK-1	Pancreatic cancer
AGS	Gastric cancer	HT1376	Bladder cancer	PK-45H	Pancreatic cancer
Alex	Liver cancer	HT17	Liver cancer	PK-45P	Pancreatic cancer
AZ-521	Gastric cancer	HT29	Colon cancer	PK-59	Pancreatic cancer
BT-474	Breast cancer	HTB49	Kidney cancer	PK-8	Pancreatic cancer
BT-483	Breast cancer	HuH28	Bile duct cancer	RPMI8226	Myeloma
C33A	Cervical cancer	HuH6	Liver cancer	RT4	Bladder cancer
CaCo-2	Colon cancer	HuH7	Liver cancer	Saos-2	Osteosarcoma
CAK12	Kidney cancer	J82	Bladder cancer	SCH	Choriocarcinoma
CAPAN-1	Pancreatic cancer	JMSU3	Bladder cancer	SF188	Glioblastoma
COLO320	Colon cancer	K-562	Leukemia	SF763	Glioblastoma
DL1	Colon cancer	KATOIII	Gastric cancer	SJSA-1	Osteosarcoma
DUI45	Prostate cancer	KLM-1	Pancreatic cancer	SK-BR-3	Breast cancer
G-361	Melanoma	LNCaP clone FGC	Prostate cancer	SK-MEL-28	Melanoma
H1299	Lung cancer	LOVO	Colon cancer	SKOV8	Ovarian cancer
H157	Lung cancer	MCF7	Breast cancer	SW480	Colon cancer
H2009	Lung cancer	MDA PCA 2b	Prostate cancer	T-47D	Breast cancer
H209	Lung cancer	MDA468	Cervical cancer	T84	Colon cancer
H2122	Lung cancer	MDA-MB-175-VII	Breast cancer	T98G	Glioblastoma
H2347	Lung cancer	MDA-MB-231	Breast cancer	TCC-SUP	Bladder cancer
H292	Lung cancer	MDA-MB-361	Breast cancer	TCS	Uterus cancer
H460	Lung cancer	MDA-MB-415	Breast cancer	TE10	Esophagus cancer
H522	Lung cancer	MDA-MB-435S	Breast cancer	TE11	Esophagus cancer
HCC1008	Breast cancer	ME180	Uterus cancer	TE14	Esophagus cancer
HCC1143	Breast cancer	MKN-1	Gastric cancer	TE4	Esophagus cancer
HCC1187	Breast cancer	MKN-45	Gastric cancer	TE6	Esophagus cancer
HCC1395	Breast cancer	MKN-45	Gastric cancer	TE8	Esophagus cancer
HCC1599	Breast cancer	NCI-H1395	Lung cancer	TE9	Esophagus cancer
HCC1937	Breast cancer	NCI-H2126	Lung cancer	TGW	Neuroblastoma
HCC1954	Breast cancer	NCI-H358	Lung cancer	THP-1	Leukemia
HCC202	Breast cancer	NCI-H526	Lung cancer	TOV-112D	Ovarian cancer
HCC2157	Breast cancer	NCI-H69	Lung cancer	U343	Glioblastoma
HCC2218	Breast cancer	NMCG1	Glioblastoma	U87	Glioblastoma
HCC38	Breast cancer	NUGC3	Gastric cancer	UACC812	Breast cancer
HCT116	Colon cancer	NUGC4	Gastric cancer	UACC893	Breast cancer
HepG2	Liver cancer	OCUM-2MD3	Gastric cancer	VMRC-RCZ	Kidney cancer
HL60	Leukemia	OV167	Ovarian cancer	WM-115	Melanoma
HLC-1	Lung cancer	OV202	Ovarian cancer	ZR-75-1	Breast cancer
		OVCAR5	Ovarian cancer	ZR-75-30	Breast cancer

Table S2. Results of Sequence Motif Analyses

Motif name	Motif sequence	Breakpoint regions				Control sequences	
		<i>PARK2</i> (n=384)	%	<i>DMD</i> (n=406)	%	(n=5,000)	%
X-element <i>E.coli</i>	GCTGGTGG	5	1.3	2	0.5	36	0.7
Ade6-M26	ATGACGT	2	0.5	5	1.2	26	0.5
ARS consensus <i>S. cerevisiae</i>	WTTTATRITTW	7	1.8	9	2.2	96	1.9
ARS consensus <i>S. pombe</i>	WRTTATTTAW	4	1.0	2	0.5	100	2.0
Consensus scaffold attachment region 1	AATAAAAYAAA	7	1.8	8	2.0	198	4.0
Consensus scaffold attachment region 2	TTWTWTTWTT	207	53.9	249	61.3	3362	67.2
Consensus scaffold attachment region 3	WADAWAYAWW	181	47.1	236	58.1	2786	55.7
Consensus scaffold attachment region 4	TWWTDTTWWW	393	102.3	469	115.5	6292	125.8
Deletion hotspot consensus	TGRRKM	728	189.6	783	192.9	9626	192.5
DNA polymerase arrest site	WGGAG	458	119.3	349	86.0	5962	119.2
DNA polymerase a frameshift hotspot 1	TCCCCC	38	9.9	30	7.4	308	6.2
DNA polymerase a frameshift hotspot 2	CTGGCG	9	2.3	6	1.5	68	1.4
DNA polymerase b frameshift hotspot 1	ACCCWR	173	45.1	146	36.0	2030	40.6
DNA polymerase a/b frameshift hotspot 1	ACCCCA	28	7.3	49	12.1	476	9.5
DNA polymerase a/b frameshift hotspot 2	TGGNGT	156	40.6	145	35.7	2244	44.9
<i>Drosophila</i> topoisomerase II consensus	GTNWAYATTNATNNR	4	1.0	2	0.5	20	0.4
Heptamer recombination signal	CACAGTG	20	5.2	15	3.7	268	5.4
Human hypervariable minisatellites sequence 1	GGAGGTGGGCAGGARG	0	0.0	0	0.0	0	0.0
Human hypervariable minisatellites sequence 2	AGAGGTGGGCAGGTGG	0	0.0	0	0.0	0	0.0
Human minisatellites core sequence	GGGCAGGARG	2	0.5	0	0.0	8	0.2
Human replication origin consensus	WAWTTDDWWDHWGWHMAWTT	0	0.0	0	0.0	8	0.2
Human minisatellites conserved sequence	GCWGGWGG	12	3.1	10	2.5	252	5.0
Ig heavy chain class switch repeat 1	GAGCT	144	37.5	127	31.3	1702	34.0
Ig heavy chain class switch repeat 2	GGGCT	101	26.3	77	19.0	1420	28.4
Ig heavy chain class switch repeat 3	GGGGT	95	24.7	90	22.2	1238	24.8
Ig heavy chain class switch repeat 4	TGGGG	144	37.5	150	36.9	2108	42.2
Ig heavy chain class switch repeat 5	TGAGC	173	45.1	143	35.2	2252	45.0
LTR-IS motif	TGGAAATCCCC	0	0.0	0	0.0	2	0.0
Mariner transposon-like element	GAAAATGAAGCTATTTACCCAGGA	0	0.0	0	0.0	0	0.0
Murine MHC recombination hotspot	CAGRCAGR	18	4.7	16	3.9	288	5.8
Murine parvovirus recombination hotspot	CTWTTY	334	87.0	405	99.8	4894	97.9
Nonamer recombination signal	ACAAAAACC	1	0.3	1	0.2	6	0.1
Pur binding site	GGNNGAGGGAGARRRR	0	0.0	1	0.2	4	0.1
Recombination hotspot	CCNCCNTNCCNC	10	2.6	4	1.0	110	2.2
Retrotransposon	TCATACACCACGCAGGGGTAGAGGACT	0	0.0	0	0.0	0	0.0
Translin binding site 1	ATGCAG	42	10.9	48	11.8	660	13.2
Translin binding site 2	GCCCWSSW	29	7.6	25	6.2	458	9.2
Vaccinia topoisomerase I consensus	YCCTT	368	95.8	419	103.2	5186	103.7
Vertebrate topoisomerase II consensus	RNYNNCNGYNGKTNINY	3	0.8	3	0.7	82	1.6
XY32 homopurine-pyrimidine H-palindrome motif	AAGGGAGAARGGGTATAGGGRAAGAGGGAA	0	0.0	0	0.0	0	0.0

Table S3. Result of the Analyses of AT Content and Flexibility Peak

Region of interest	Position	AT content (%)	Average twist angle (degree)	Flexibility peak (peaks/Mb) ^{a)}	Unified peak (peaks/Mb) ^{b)}	Cluster of peaks (peaks/Mb) ^{c)}
	chromosome 6: 159,870,000-160,370,000	56.70	10.66	40	26	4
	chromosome 6: 160,370,000-160,870,000	56.90	10.70	32	18	4
	chromosome 6: 160,870,000-161,370,000	59.43	10.81	44	36	4
	chromosome 6: 161,370,000-161,870,000	56.98	10.68	52	32	8
	chromosome 6: 161,870,000-162,370,000	59.16	10.85	74	44	10
Breakpoint clustering region	chromosome 6: 162,370,000-162,870,000	60.66	10.90	50	24	0
	chromosome 6: 162,870,000-163,370,000	61.86	10.96	64	32	8
	chromosome 6: 163,370,000-163,870,000	58.61	10.74	32	24	4
	chromosome 6: 163,870,000-164,370,000	57.59	10.72	36	26	4
	chromosome 6: 164,370,000-164,870,000	60.67	10.87	104	46	12
	chromosome 6: 164,870,000-165,370,000	62.64	11.03	88	50	12
	chromosome X: 29,000,000-29,500,000	63.70	11.08	116	56	18
	chromosome X: 29,500,000-30,000,000	63.22	11.07	72	50	10
	chromosome X: 30,000,000-30,500,000	61.32	10.92	36	24	4
	chromosome X: 30,500,000-31,000,000	59.65	10.81	56	38	6
	chromosome X: 31,000,000-31,500,000	61.19	10.89	34	30	0
Breakpoint clustering region	chromosome X: 31,500,000-32,000,000	63.96	11.07	52	40	2
	chromosome X: 32,000,000-32,500,000	64.69	11.15	100	62	14
	chromosome X: 32,500,000-33,000,000	63.76	11.12	80	56	8
	chromosome X: 33,000,000-33,500,000	64.18	11.13	100	66	18
	chromosome X: 33,500,000-34,000,000	64.44	11.11	78	42	12
	chromosome X: 34,000,000-34,500,000	63.77	11.08	82	50	12

^{a)} Average twist angles ≥ 13.7 were considered.

^{b)} Distance between adjacent peaks ≤ 100 bp was unified.

^{c)} Equal or more than 3 unified peaks whose distance between adjacent unified peaks are smaller than 5,000 bp.